Fluoroscopy Simulation of a Mobile C-arm

600.446. Computer Integrated Surgery II

Group 5: Seung Wook Lee, Ju Young Ahn

Mentors: Dr. Jeff Siewerdsen, Dr. Matthew Jacobson, Dr. Tharindu De Silva, Dr. Joseph Goerres

May 6, 2016

Contents

1. Introduction

Mobile C-arm is an X-ray imaging device with a flexible positioning of its X-ray source. This device is widely used as a means of providing fluoroscopy-based surgical guidance in many areas including orthopedic surgeries. Multiple degrees of freedom (DOF) of the C-arm with angular and orbital movements allow surgeons to set an optimal viewpoint for surgeries.

However, placing the C-arm to the preferred position often requires surgeons to take multiple fluoroscopic shots to find an optimal view. This process is time-consuming and increases radiation exposures to both patients and surgeons. Also, this process is physically cumbersome and requires skills for surgeons to manually maneuver the C-arm.

http://www.simeks.com.tr/en/portfolio-item/siemens-cios-alpha/

Figure 1. Cios-alpha (left), Fluoroscopic images of the same object with two different viewpoints (Right)

There are several challenges to be addressed in this project. One is modeling of C-arm geometry. C-arm has multiple degrees of freedom (DOFs) with angular and orbital movements. However, its orbital trajectories are not isocentric and perfectly circular geometry could not be assumed for orbital movements. As a result, additional calibration steps are required. Also, our initial approach to register patient to 3D CT volume using an optical tracking system shows several weaknesses; optical tracker used in our project has a limited field of view, incapable of capturing full motion of C-arm gantry. Also, usage of the optical tracker is disjointed from surgical workflows. Thus, we decide to perform 3D-2D image registration to get rid of optical trackers and to increase compatibility of the module with surgical workflow.

Here, we propose a system capable of optimal positioning of the C-arm based on digitally reconstructed radiograph (DRR) to solve the problems associated with the process of finding the optimal view. We expect several advantages using this DRR-driven user interface. Since our guidance of the C-arm is based on radiation-free fluoroscopic previews, it is less time consuming and has minimal radiation exposure to both surgeons and patients. Also, we expect to have less user variability and more consistency using our system.

In order to validate our interfaces, we compared generated DRR images to actual fluoroscopic images taken by Cios-alpha (*Figure 1*) using several criterions including projection distance error (PDE) and image intensity differences. PDE results were under 3.5 mm for angular movements and under 8 mm for orbital movements. Image intensity differences were under 0.3 for both angular and orbital movements.

2. Technical Approaches

2.1 DRR generation

To generate DRR, we used the Siddon forward projection method for ray tracing in a previously acquired CT image of the patient[1]. The algorithm to generate DRR was built by one of our mentors in I-STAR Lab. Where a number of rays radiate from a source to a detector, position of a ray on the detector is computed based on projection geometry. Then equidistant points are placed along the line connecting the source position and the position of a ray on the detector based on linear interpolation. Based on attenuation value of a voxel where each point falls in, attenuation of each point is computed and attenuation of a ray is defined as a sum of the attenuation value of the points. This method, accelerated by GPU, has an advantage in DRR generation speed, which is important to be well-integrated with surgical workflow.

2.2 Registration

One method to register the C-arm, CT image, and patient is using a surgical tracker (Polaris Spectra) and fiducial marker. However, the typical tracker field of view is too small to cover the full movement of the C-arm, and such systems tend to introduce cumbersome workflow with limited clinical acceptance in broad application.

As a solution, we decided to perform 3D-2D image registration to define relative positions between patients and the C-arm. We used 3D-2D image registration software available in the I-STAR lab to acquire relative positions between C-arm and patient[2]. This 3D-2D image registration used a single fluoroscopic image of the phantom. With knowledge of C-arm geometry, transformation matrix that best corresponds a DRR with the fluoroscopic image was computed.

A surgical tracker could similarly be used to calibrate the C-arm geometry. For similar reasons as noted above, we preferred a method that operates without trackers. As a result, we decided to define source and detector positions at each angle using software called “GeoCalc,” developed by one of our mentors in the I-STAR Lab. Using this software, information of C-arm

geometry, such as source or detector positions, at different purely angular or orbital positions was acquired. By purely angular or orbital positions, we mean orbital or angular position with the other position fixed at zero. The reason that the calibration data was collected for the purely angular or orbital movement lies in difficulties in anticipating all possible trajectories. The matrices are acquired for the full 360 degrees for angular movements. Due to non-isocentricity of the C-arm's orbital movement, calibration object did not stay in the scene for full 180°. Therefore, the matrices for pure orbital movements are collected within a predefined range of -40° to 20°. With the registration and calibration data, we could generate digitally reconstructed radiograph (DRR) with high accuracy.

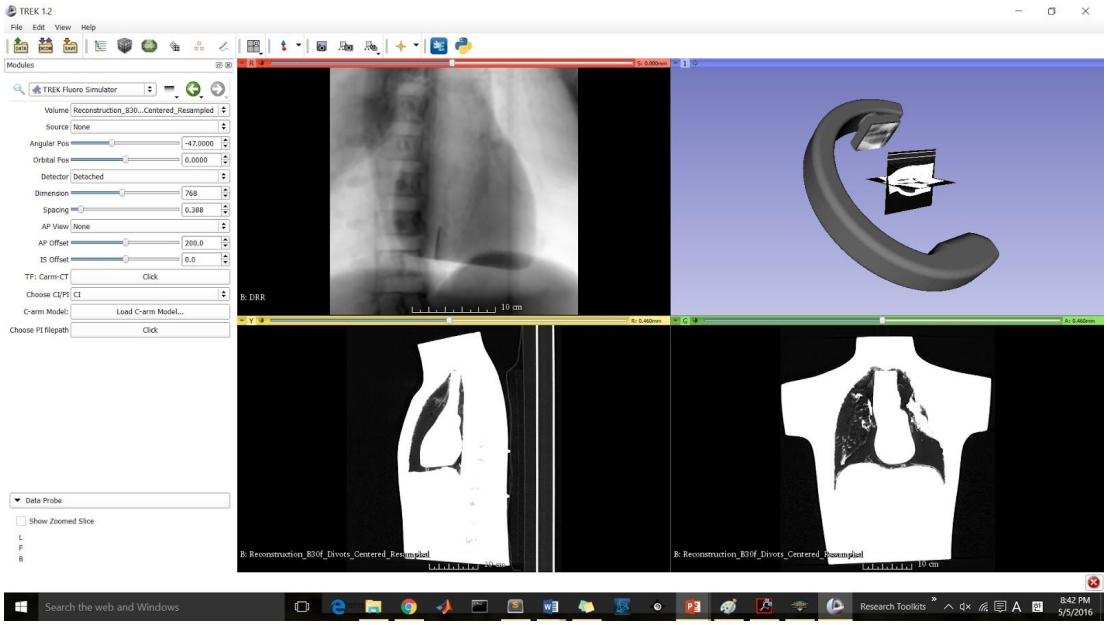

Figure 2.1. Module design with control panel, corresponding DRR, and 3D space.

2.3 UI development: Computer Interface (CI)

One of the user interfaces that we developed is computer interface (CI). Computer interface takes in registration data and allows visualization of DRR as the operator manipulates angular and orbital positions of the source using sliders in the module. In terms of interface development, a model of C-arm's 3D volume is loaded using a STL (STereoLithography) file (*Figure 2.1*). This model of C-arm is rotated simultaneously according to the angular and orbital degrees specified by the user. Also, we noticed that the generated DRR images had too bright or too dark regions and some anatomical structures were hard to visualize. As a solution, we specified the color map grayscale level to prevent saturation of DRR images. As a result, in addition to being less time consuming, and exposing less radiation, computer interface has

several additional advantages. The user will not be required to maneuver the C-arm, which can be physically cumbersome; the user only has to modify angular and orbital degrees and simulated DRR will be displayed on the screen without any fluoro shots. Then, when the optimal viewpoint is determined, the user would have to move the C-arm to that position and take a fluoroscopic image.

Figure 2.2. Generation of DRR based on C-arm position

2.4 UI development: Physical Interface (PI)

We further developed computer interface to detect a physical posture of C-arm, thereby establishing physical interface (PI). The physical interface takes in registration data and an input .txt file that contains real-time angular and orbital position information and then it simulates DRR as the operator maneuvers the C-arm to find an optimal viewpoint just as if he or she would have done in actual surgeries. In terms of interface development, we added a selection toolbar, set to be either computer interface (default) or physical interface. When the user chooses the physical interface, a dialog box is popped and the user can select the input .txt file to read angular and orbital information. A built-in software of Cios-alpha is used to store angular and orbital information into a text file. Then, as the user moves the C-arm position, our module reads in angular and orbital values and display DRR in accordance (*Figure 2.2*). This DRR generation has a frame rate of 1 frame per second (fps) as it is updated every second. The frame rate is adjustable to be faster. Primary limiting factor of the frame rate is performance of a computer. Physical interface has a significant advantage over computer interface that it seamlessly integrates into the surgical procedure since the user still maneuvers C-arm in search of an optimal viewpoint without radiation exposure.

Detailed information and instruction on the UI can be found in the user manual which is linked as an appendix.

3. Result/ Validation

We evaluated the accuracy of our system by comparing DRR and actual radiographs. Fluoroscopic images of a phantom were taken at 10 different purely orbital and angular positions. We took DRRs using 3D CT volume of the phantom (512 x 512 x 641) at the same orbital and angular positions in a digital space.

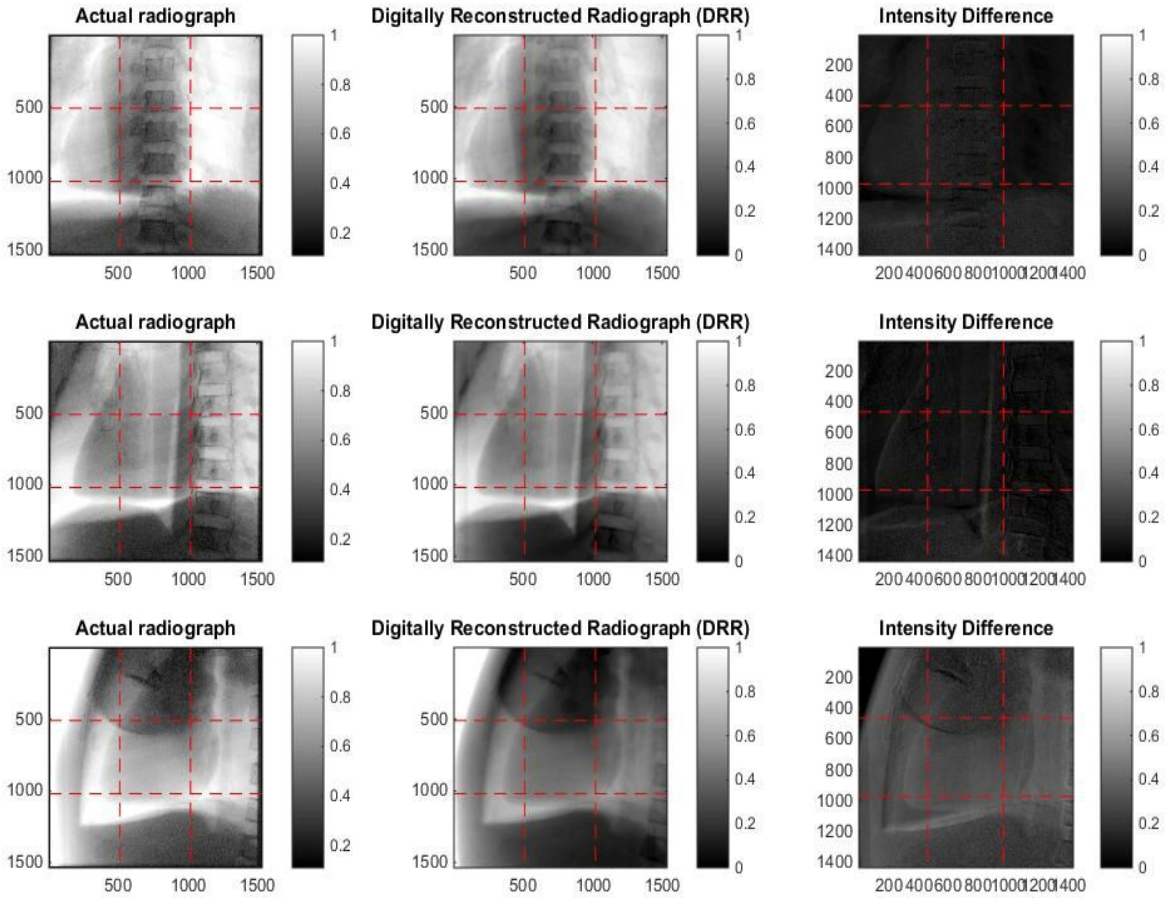

Figure 3. Comparison between real radiograph (left), DRR (middle), and normalized intensity difference (right)

Figure 3 provides images of actual radiographs and DRRs at purely angular positions of 0, 15 and 60 degrees. Although there are differences in contrast and resolution, similarities between the two sets of images could be observed. The DRR had relatively lower resolution compared to actual radiograph as a resolution of the DRR is primarily governed by resolution of preoperative CT scan and linear interpolation method is used to generate DRR. To quantify the similarities between the two sets of images, we measured projection distance error (PDE) and intensity difference between the two sets of images.

3.1 Projection Distance Error (PDE)

Angles (°)	-30	-15	0	9	15	30	45	60	75	90
Angular PDE (mm)			1.7901		1.2916	1.7817	2.2816	2.8035	2.894	3.809
Orbital PDE (mm)	6.2858	5.4827	1.7901	5.9164						

Table 1. PDE at different pure angular and orbital positions of the C-arm

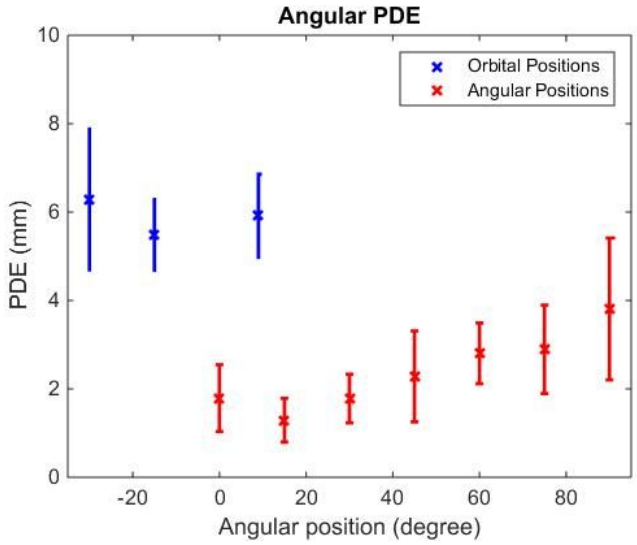

Figure 3.1. Plot of PDE for different pure angular and orbital positions of the C-arm

For each purely angular and orbital positions, PDE between actual fluoroscopic image and DRR is computed. Pixel positions of 16 different landmarks are collected from each image. Distances between the points representing the same landmark are computed and converted to millimeter (pixel size = 0.192 mm/pixel). PDE was on average 2.3788 mm for purely angular positions and 5.8950 mm for purely orbital positions (*Table 1 and Figure 3.1*). This result suggests that our system is capable of simulating fluoroscopic image under 10 mm of translational error.

The PDEs are not consistent and increase as orbital or angular position deviates from zero. A reason for this trend lies on our 3D-2D registration. The 3D-2D registration used in the experiment was done based on a single fluoroscopic shot taken at zero position. Therefore, the registration may not be as accurate in depth direction. If the registration was done with more fluoroscopic shots, the registration would have been more accurate in depth direction, thereby removing trend of PDE.

One of the possible reasons that PDE is higher for a purely orbital position could be explained with in terms of a correspondence of two sets of geometric calibration. Two calibration

processes for purely angular (full 360°) and orbital (-40° ~ +20°) positions are performed. But as the two calibrations are done separately, a process to match a home position of the two calibrations is required. However, the match is not completely accurate and this error in correspondence between the two calibration data might introduce an additional error in PDE in purely orbital positions.

3.2 Intensity Difference

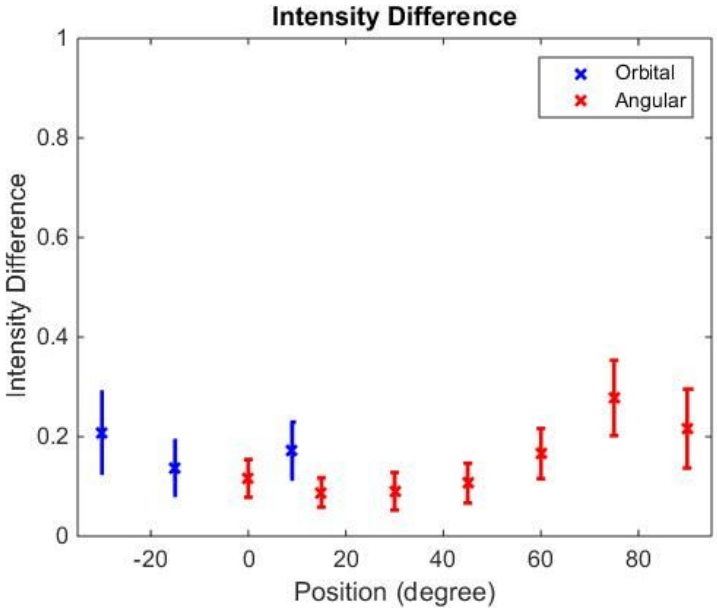

Figure 3.2. Intensity differences at different pure angular and orbital positions of the C-arm

Angles (°)	-30	-15	0	9	15	30	45	60	75	90
Angular Intensity Difference			0.1161		0.0878	0.0903	0.1065	0.166	0.2779	0.2162
Orbital Intensity Difference	0.2081	0.1371	0.1161	0.1721						

Table 2. Intensity differences at different pure angular and orbital positions of the C-arm

To measure intensity difference, actual fluoroscopic images and DRRs at different angles are normalized and subtracted. 50 pixels are cropped from each side of the images as detector frame of the C-arm was captured in the cropped area. Hence, images with an area of interest (AOI) 1436 x 1436 was used to compute the intensity differences. The right column of Figure 3 displays intensity difference images, and Figure 3.2 plots mean intensity differences at different pure angular and orbital positions. The average difference was 0.1578, and the difference was similar for both purely angular and orbital positions (Table 2 and Figure 3.2). Similarities of intensities between DRR and actual fluoroscopic image is another metric validating our result. Although PDE between the images did contribute to the intensity

differences, Figure 3 suggests saturation of actual fluoroscopic image as a main source of the difference. In the figure, background or the area between lung and diaphragm is much brighter than DRR in actual fluoroscopy. That image of intensity differences models is higher when more background is present suggest a contribution of the saturation in intensity differences.

4. Significance

Surgeons who regularly utilize the C-arm for their surgeries are continuously endangered to radiation exposure. Moreover, the process of finding an optimal viewpoint for the C-arm delays surgical procedures is physically cumbersome and is dependent on the operator's skills. Our user interfaces resolve these problems by simulating digitally reconstructed radiograph (DRR) from preoperative 3D CT volume. Using these interfaces, surgeons would be exposed to less or no radiation, and procedure would be less delayed as surgeons no longer need to take multiple fluoroscopic images to find an optimal view. Moreover, since our interfaces adopt 3D-2D image registration, instruments other than the C-arm, such as optical tracking system, that might obstruct surgical workflow is not required.

The computer interface allows visualization of DRR with easy modification of angular and orbital position sliders. The physical interface allows real-time display of DRR in accordance with the actual C-arm position, thereby coherently integrating into surgical procedures.

We validated our interfaces by comparing results of DRR to actual fluoroscopic images. Projection distance error (PDE) was calculated by pinpointing anatomical landmarks and measuring the distance differences. Also, image intensity difference was measured by normalizing image gradients of DRR and fluoroscopy and subtracting from one another. Our interfaces produced accurate DRR images as PDE was less than 3.5 mm and 8 mm for angular orbital movements, respectively, and image intensity difference was under 0.3 for both angular and orbital movements.

5. Management Summary

5.1 Responsibilities

We worked together throughout the project. Both members participated in the development of module within 3D Slicer, data collection, and validation of experimental results.

5.2 Plan vs. Accomplishments

Our original plan was to develop an algorithm involving an optical tracking system to register the patient, C-arm, and CT volume as a minimum deliverable. The algorithm is developed, yet is not used for actual experiments as using 3D-2D registration present in the I-STAR Lab could better integrate with surgical workflow. Instead, we used 3D-2D registration algorithm, of which incorporation was planned to be one of our maximum deliverables, for registration.

In terms of accomplishments, we were able to complete all minimum, expected, and maximum deliverables with an exception of one maximum deliverable which was to automate C-arm movement using SITA interface (Table 3). We decided not to pursue this deliverable and focused our attention on the further development of physical interface because PI could seamlessly integrate into surgical procedures and was a more valuable achievement.

Deliverables	Status
Minimum deliverables	Completed
Registration: CT-Phantom using optical trackers	Completed
Registration: C-arm using optical trackers	Completed
Modify DRR generation module to represent source position in angular/orbital position	Completed
Expected deliverables	Completed
Physical Interface, capable of acquiring real-time C-arm position and displaying DRR	Completed
Computer Interface, capable of specifying virtual C-arm position and displaying DRR	Completed
Maximum deliverables	Completed
CT-Phantom registration with 3D-2D image registration	Completed
Computer Interface – Drive the C-arm to preferred position by SITA interface	Not pursued

Table 3. Deliverables and their status

5.3 Future Plan

Even though we were able to achieve accurate DRR compared to an actual fluoroscopic image, the trajectories were limited to either purely angular or orbital movements. Thus, development of more accurate modeling of C-arm geometry to account for non-isocentricity of C-arm would allow accurate DRR generation at a mixed angular/orbital position.

Currently, our module utilizes several softwares to generate DRR. These softwares are 3D-2D image registration software, GeoCalc software, and software to read and store angular/orbital information of C-arm and they are all in separate platforms. Our future step would be to integrate these different softwares into one single module.

Even though our PDE values were less than 3mm and 8mm for angular and orbital movements respectively, it is discussed (in Result/ Validation section) that PDE values for orbital movements were consistently higher than those for angular movements. For future work, we could investigate several hypotheses for this discrepancy. One hypothesis is that geometric calibration data for orbital angles are not completely accurate due to its non-isocentric orbits. Also, we hypothesized that orbital angle information could be more precisely approximated by fitting an ellipse to an orbital trajectory and interpolating the orbital locations.

5.4 Lesson Learned

From this project, we learned about camera/CT projection geometry and had valuable experiences in software development using TREK. We learned the importance of validation processes. Through validation processes, we were able to examine our module, discover any necessary revisions, and improve the quality of our module. We also learned the importance of communications with mentors and between partners. Moreover, since we utilized several softwares, we learned the importance of matching coordinate systems among different programs.

5.5 Acknowledgements

We would like to thank our mentors Dr. Matthew Jacobson, Dr. Joseph Goerres, Dr. Tharindu De Silva, and professor Dr. Jeff Siewerdsen for valuable advice and providing 3D-2D registrations, geographical calibration, and software to read and write C-arm encoder values. In addition, we would like to thank Ali Uneri who provided us step-by-step guidance in an installation of TREK on our local devices and instructions on UI development. .

6. Technical Appendices

Our codes for the module are stored in git repository used by I-STAR lab.
Link is provided: https://git.lcsr.jhu.edu/groups/istar (on Wiki page as well)
Our codes to compute PDE and intensity differences for validation of DRRs are uploaded to the git repository. Link is provided: https://github.com/slee333/CISII (on Wiki page as well)

The user manual for the system we developed (named ‘FluoroSim’) is uploaded to the WIki Page for convenience of a user and for the purpose of documentation.

7. Reference

[1] Siddon, Robert L. "Fast Calculation of the Exact Radiological Path for a Three-dimensional CT Array." *Med. Phys. Medical Physics* 12.2 (1985): 252. Web.

[2] *Uneri, A. et al. “Known-Component 3D-2D Registration for Image Guidance and Quality Assurance in Spine Surgery Pedicle Screw Placement.”Proceedings of SPIE--the International Society for Optical Engineering 9415 (2015): 94151F. PMC. Web.*